Research Article

Nonlinear Adaptive Equivalent Control Based on Interconnection Subsystems for Air-Breathing Hypersonic Vehicles

Chaofang Hu and Yanwen Liu

School of Electrical Engineering and Automation, Tianjin University, Tianjin 300072, China

Correspondence should be addressed to Chaofang Hu; cfhu@tju.edu.cn

For the nonminimum phase behavior of the air-breathing hypersonic vehicle model caused by elevator-to-lift coupling, a nonlinear adaptive equivalent control method based on interconnection subsystems is proposed. In the altitude loop, the backstepping strategy is applied, where the virtual control inputs about flight-path angle and attack angle are designed step by step. In order to avoid the inaccurately direct cancelation of elevator-to-lift coupling when aerodynamic parameters are uncertain, the real control inputs, that is, elevator deflection and canard deflection, are linearly converted into the equivalent control inputs which are designed independently. The reformulation of the altitude-flight-path angle dynamics and the attack angle-pitch rate dynamics is constructed into interconnection subsystems with input-to-state stability via small-gain theorem. For the velocity loop, the dynamic inversion controller is designed. The adaptive approach is used to identify the uncertain aerodynamic parameters. Simulation of the flexible hypersonic vehicle demonstrates effectiveness of the proposed method.

1. Introduction

Hypersonic vehicles have a promising prospect in both military and commercial applications as its flight speed can be more than 5 times of the speed of sound. However, since the model of hypersonic vehicle is nonlinear, multivariable, uncertain, and coupling [1], it is unstable and extremely sensitive to changes in flight condition and parameters. This brings a great challenge to controller design [2]. At present, most researches focus on dealing with nonlinearity and uncertainty of hypersonic vehicles. For example, linear control methods are attempted according to linearized hypersonic vehicle models, such as pole placement techniques [3], LQR method [4], linear output feedback control [5], and LPV control [6]. In addition, nonlinear control strategies are widely used as well, such as feedback linearization approach [7], sliding control [8, 9], and backstepping technique [10]. For uncertainty of hypersonic vehicles, besides adaptive approaches [11], robust strategies are common tools, for example, μ-synthesis, H_∞ control [12], stochastic robustness control [13], and nonlinear disturbance observer-based robust control

[14]. Although these methods are proven to be effective, they do not usually consider the coupling problems existing in hypersonic vehicles. These problems lead to more difficulties in the flight controller design. In an air-breathing hypersonic vehicle, it is known that there are structural dynamics, flexible effect, elevator-to-lift coupling, and the coupling between thrust and pitch moment, where elevator-to-lift coupling is not neglectable, and it will generate unstable zero dynamics exponentially, that is, the nonminimum phase behavior in pitch rate model, if the controller is designed directly by the inversion.

With regard to the elevator-to-lift coupling problem, some strategies have been tried. The basic method usually ignores this coupling, and then the nonminimum phase can be removed from the model during the controller design [2], where this coupling is only regarded as unmodeled dynamics. However, this manner cannot ensure the stability of the control system. The other common approach is to offset the influence of the coupling. For example, a canard is adopted to cancel the influence of elevator on lift, and an adaptive robust controller based on nonlinear sequential loop-closure

approach is developed [15, 16]. Nevertheless, the changes of the uncertain parameters are not considered. This may result in the inaccurate cancellation, which means elevator and lift are not decoupled completely. Simultaneously, this approach has an adverse influence on the pitch rate dynamics since its inputs also consist of elevator and canard. In addition, for thermal protection problem resulted from the canard, only the elevator is taken as aerodynamic control surface in reference [17]. The system model is transformed into the interconnection of systems in feedback and feedforward forms to eliminate the nonminimum phase. But the robustness with regard to uncertainty of the hypersonic vehicle model is not addressed totally.

From the analysis, we know that adding canard control surface is an effective and simple way to suppress the nonminimum phase behavior, even though the strict cancellation of the elevator-to-lift coupling cannot be realized actually. In this paper, the flexible air-breathing hypersonic vehicle model is considered. For the tracking requirement of altitude and velocity, a nonlinear adaptive equivalent control method based on interconnection subsystems is proposed by incorporating canard. Firstly, in the altitude loop, the virtual control inputs about flight-path angle and attack angle are designed step by step according to the backstepping strategy. Secondly, the terms about the real control inputs, that is, the elevator and canard deflection in the flight-path angle dynamics and the pitch rate dynamics, are linearly converted into the equivalent control inputs instead of direct cancelation of the elevator-to-lift coupling. By designing the new inputs independently, the altitude control loop is reformulated. And the adaptive technique is used to identify the uncertain aerodynamic parameters. Then the interconnection subsystems including the altitude-flight-path angle dynamics and the attack angle-pitch rate dynamics are constructed. Via the small-gain method, the system is proven to be input-to-state stable. In the velocity loop, the adaptive dynamic inversion controller is designed. Simulation results show the power of our approach.

In Section 2, the air-breathing hypersonic vehicle model is presented. The nonlinear adaptive equivalent control based on interconnection subsystems is introduced in Section 3. Section 4 presents the simulation. The conclusion is drawn in Section 5.

2. Air-Breathing Hypersonic Vehicle Model

In this study, the flexible air-breathing hypersonic vehicle model [18] is considered. This model is composed of five rigid-body states, that is, velocity V, altitude h, flight-path angle γ, attack angel α, pitch rate q, and six flexible states, that is, η_1, $\dot{\eta}_1$, η_2, $\dot{\eta}_2$, $\dot{\eta}_3$, and $\dot{\eta}_3$. The equations of motion are written as

$$\dot{V} = \frac{T\cos\alpha - D}{m} - g\sin\gamma,$$

$$\dot{h} = V\sin\gamma,$$

$$\dot{\gamma} = \frac{T\sin\alpha + L}{mV} - \frac{g\cos\gamma}{V},$$

$$\dot{\alpha} = Q - \dot{\gamma},$$

$$\dot{Q} = \frac{M}{I_{yy}},$$

$$\ddot{\eta}_i = -2\varsigma_m\omega_{m,i}\dot{\eta}_i - \omega_{m,i}^2\eta_i + N_i; \quad i = 1, 2, 3,$$

(1)

where m, I_{yy}, g represent mass of the aircraft, moment of inertia, gravitational acceleration; damping ratio and natural frequency of the flexible motion are denoted by ς_m and $\omega_{m,i}$, respectively; T, D, L, and N_i and M are thrust, drag, lift, generalized forces and moment

$$L = \bar{q}SC_L,$$

$$T = \bar{q}\left(C_{T,\phi}\phi + C_T\right),$$

$$D = \bar{q}SC_D,$$

$$M = z_T T + \bar{q}S\bar{c}C_M,$$

$$N_i = \bar{q}C_{N_i}.$$

(2)

The aerodynamic parameters in the above formulation are described as follows:

$$C_L = C_L^\alpha \alpha + C_L^{\delta_e}\delta_e + C_L^{\delta_c}\delta_c + C_L^0 + C_L^{\Delta\tau_1}\Delta\tau_1 + C_L^{\Delta\tau_2}\Delta\tau_2,$$

$$C_M = C_M^\alpha \alpha + C_M^{\delta_e}\delta_e + C_M^{\delta c}\delta_c + C_M^0 + C_M^{\Delta\tau_1}\Delta\tau_1 + C_M^{\Delta\tau_2}\Delta\tau_2,$$

$$C_{N_i} = C_{N_i}^\alpha \alpha + C_{N_i}^{\delta_e}\delta_e + C_{N_i}^{\delta_c}\delta_c + C_{N_i}^0 + C_{N_i}^{\Delta\tau_1}\Delta\tau_1 + C_{N_i}^{\Delta\tau_2}\Delta\tau_2,$$

$$C_D = C_D^{(\alpha+\Delta\tau_1)^2}\left(\alpha+\Delta\tau_1\right)^2 + C_D^{(\alpha+\Delta\tau_1)}\left(\alpha+\Delta\tau_1\right) + C_D^{\Delta\tau_2}\Delta\tau_2$$

$$+ C_D^{\delta_e^2}\delta_e^2 + C_D^{\delta_e}\delta_e + C_D^{\alpha\delta_e}\alpha\delta_e + C_D^{\delta c^2}\delta_c^2$$

$$+ C_D^{\delta_c}\delta_c + C_D^{\alpha\delta_c}\alpha\delta_c + C_D^0,$$

$$C_{T,\phi} = C_{T,\phi}^\alpha \alpha + C_{T,\phi}^{\alpha M_\infty^{-2}}\alpha M_\infty^{-2} + C_{T,\phi}^{M_\infty^{-2}} M_\infty^{-2} + C_{T,\phi}^0$$

$$+ C_{T,\phi}^{\alpha\Delta\tau_1}\alpha\Delta\tau_1 + C_{T,\phi}^{\Delta\tau_1^2}\Delta\tau_1^2 + C_{T,\phi}^{\Delta\tau_1}\Delta\tau_1,$$

$$C_T = C_T^\alpha \alpha + C_T^{M_\infty^{-2}} M_\infty^{-2} + C_T^{A_d} A_d + C_T^{\Delta\tau_1}\Delta\tau_1 + C_T^0,$$

(3)

where the control inputs are fuel-to-air ratio ϕ, elevator deflection δ_e, and canard deflection δ_c; $\bar{q}$, S, z_T, $\bar{c}$, M_∞ denote dynamic pressure, reference area, thrust moment arm, mean aerodynamic chord, and Mach number; $\Delta\tau_1$ and $\Delta\tau_2$ are the forebody turn angle and the aftbody vertex angle which are linear mapping of elastic states η_i.

In (3), the elevator-to-lift coupling orients from that C_L includes the term of δ_e, which leads to the nonminimum phase behavior. If δ_e is designed by the dynamic inversion directly, the pitch rate dynamics will become a hyperbolic saddle equilibrium. This unstable zero dynamic brings great difficulties to the controller design.

3. Nonlinear Adaptive Equivalent Controllers Design

In order to track the altitude and velocity command signals h_{ref} and V_{ref}, two controllers will be designed independently for the altitude loop and the velocity loop. During the controller design, the flexible motion is viewed as external perturbation, and its influence on aerodynamic model (3) is neglected.

3.1. Altitude Controller. In the altitude loop, the controller is designed according to the backstepping approach. Then the virtual control inputs about flight-path angle and attack angle are determined, respectively.

For the altitude dynamics, let $\tilde{h} = h - h_{\text{ref}}$; then its error dynamics is written in the following:

$$\dot{\tilde{h}} = V \sin \gamma - \dot{h}_{\text{ref}} \approx V\gamma - \dot{h}_{\text{ref}}. \tag{4}$$

So the flight-path angle command γ_d is designed into the following equation:

$$\gamma_d = \frac{-k_{\tilde{h}}\tilde{h} + \dot{h}_{\text{ref}}}{V}, \tag{5}$$

where $k_{\tilde{h}} > 0$ is the design parameter for $\tilde{h}$.

Let $\tilde{\gamma} = \gamma - \gamma_d$; the error dynamic of flight-path angle is presented as follows:

$$\dot{\tilde{\gamma}} = \frac{T \sin \alpha + L}{mV} - \frac{g \cos \gamma}{V} - \dot{\gamma}_d. \tag{6}$$

Here, the thrust is described as the function about the attack angle. Define $T = \nabla T\alpha + T_0$, where $\nabla T = \bar{q}(C_{T,\phi}^{\alpha M_\infty^{-2}} M_\infty^{-2}\phi + C_{T,\phi}^\alpha \phi + C_T^\alpha)$ and $T_0 = \bar{q}(C_{T,\phi}^{M_\infty^{-2}} \phi M_\infty^{-2} + C_{T,\phi}^0 \phi + C_T^{M_\infty^{-2}} M_\infty^{-2} + C_T^{A_d} A_d + C_T^0)$. As the variation range of the attack angle is small, (6) will be expanded around the final expectation α^*.

To handle the nonminimum phase problem, the MIMO equivalent method is applied in this paper, which is different from the previous research results [17]. The terms about the elevator and canard deflection are linearly equivalent to the control input vector $\mathbf{U} = [U_1, U_2]$. The error model of the flight-path angle (6) can be rewritten as

$$
\begin{aligned}
\dot{\tilde{\gamma}} &= \frac{\nabla T\alpha \sin \alpha + T_0 \sin \alpha + \bar{q}SC_L^\alpha \alpha}{mV} + \bar{q}S\frac{C_L^{\delta_e}\delta_e}{mV} + \bar{q}S\frac{C_L^{\delta_C}\delta_C}{mV} \\
&\quad + \frac{\bar{q}SC_L^0 - mg \cos \gamma - mV\dot{\gamma}_d}{mV} \\
&= \underbrace{\frac{\nabla T \sin \alpha^* + \nabla T\alpha^* \cos \alpha^* + T_0 \cos \alpha^* + \bar{q}SC_L^\alpha}{mV}}_{C_1} \alpha + \underbrace{\bar{q}S\frac{C_L^{\delta_e}\delta_e + C_L^{\delta_c}\delta_c}{mV}}_{U_1} \\
&\quad + \underbrace{\frac{\bar{q}SC_L^0 - mg \sin \gamma - mV\dot{\gamma}_d}{mV} + \frac{T_0 \sin \alpha^* - (\nabla T\alpha^* \cos \alpha^* + T_0 \cos \alpha^*)\alpha^*}{mV}}_{\beta_1} \\
&= C_1\alpha + U_1 + \beta_1,
\end{aligned} \tag{7}
$$

where C_1 and β_1 are the terms containing the uncertain aerodynamic parameters. They can be expressed as the following equations:

$$C_1 = \theta_1^T\xi_1,$$
$$\beta_1 = \theta_1^T\xi_2 - \frac{g \cos \gamma}{V} - \dot{\gamma}_d, \tag{8}$$
$$U_1 = \theta_2^T\xi_3.$$

θ_1, θ_2 are vectors of the uncertain parameters

$$\theta_1 = \left[C_{T,\phi}^\alpha; C_T^\alpha; C_{T,\phi}^{\alpha M_\infty^{-2}}; C_{T,\phi}^{M_\infty^{-2}}; C_{T,\phi}^0; C_T^{M_\infty^{-2}}; C_T^{A_d}; C_T^0; C_L^\alpha; C_L^0\right],$$
$$\theta_2 = \left[C_L^{\delta_e}; C_L^{\delta_c}\right],$$
$$\tag{9}$$

and $\xi_1, i = 1 \ldots 3$ are regressors

$$\xi_1 = \frac{\bar{q}}{mV} \Big[(\sin \alpha^* + \alpha^* \cos \alpha^*)\phi; (\sin \alpha^* + \alpha^* \cos \alpha^*);$$
$$(\sin \alpha^* + \alpha^* \cos \alpha^*)M_\infty^{-2}\phi; \cos \alpha^* M_\infty^{-2}\phi;$$
$$\cos \alpha^*\phi; \cos \alpha^* M_\infty^{-2}; \cos \alpha^* A_d; \cos \alpha^*; S; 0\Big],$$

$$\xi_2$$
$$= \frac{\bar{q}}{mV} \Big[-\alpha^{*2} \cos \alpha^*\phi; -\alpha^{*2} \cos \alpha^*; -\alpha^{*2} \cos \alpha^* M_\infty^{-2}\phi;$$
$$(\sin \alpha^* - \alpha^* \cos \alpha^*)M_\infty^{-2}\phi; (\sin \alpha^* - \alpha^* \cos \alpha^*)\phi;$$
$$(\sin \alpha^* - \alpha^* \cos \alpha^*)M_\infty^{-2}; (\sin \alpha^* - \alpha^* \cos \alpha^*)A_d;$$
$$(\sin \alpha^* - \alpha^* \cos \alpha^*); 0; S\Big],$$

$$\xi_3 = \frac{\bar{q}S}{mV} [\delta_e; \delta_c]. \tag{10}$$

Therefore the dynamics (7) is reformulated as

$$\dot{\tilde{\gamma}} = \theta_1^T\xi_1\alpha + \theta_2^T\xi_3 + \theta_1^T\xi_2 - \frac{g \cos \gamma}{V} - \dot{\gamma}_d. \tag{11}$$

Then the virtual command of the attack angle is chosen as $\alpha_d = \alpha^* - \tilde{\gamma}$.

Let $\tilde{\alpha} = \alpha - \alpha_d$; the error dynamic of the attack angle is formulated as

$$\dot{\tilde{\alpha}} = Q - \dot{\gamma} - \dot{\alpha}_d = Q - \dot{\gamma}_d. \tag{12}$$

A new variable Z is defined as $Z = Q - \dot{\gamma}_d + k_{\tilde{\alpha}}\tilde{\alpha}$, where $k_{\tilde{\alpha}} > 0$ is a design parameter for $\tilde{\alpha}$. Then (12) is rewritten as

$$\dot{\tilde{\alpha}} = Z - k_{\tilde{\alpha}}\tilde{\alpha}. \tag{13}$$

Using the equivalent control method, the time derivative of Z can be formulated with the new input U_2. It includes the pitch rate dynamics

$$
\begin{aligned}
\dot{Z} &= \frac{z_T T + \bar{q}S\bar{c}C_M}{I_{yy}} + k_{\tilde{\alpha}}\dot{\tilde{\alpha}} \\[2mm]
&= \bar{q}S\bar{c}\underbrace{\frac{C_M^{\delta_e}\delta_e + C_M^{\delta_c}\delta_c}{I_{yy}}}_{U_2} + \underbrace{\frac{z_T\nabla T + \bar{q}S\bar{c}C_M^{\alpha}}{I_{yy}}\alpha}_{C_2} \\[2mm]
&\quad + \underbrace{\frac{z_T T_0 + \bar{q}S\bar{c}C_M^0}{I_{yy}} + k_{\tilde{\alpha}}\dot{\tilde{\alpha}} - \ddot{\gamma}_d}_{\beta_2} \\[2mm]
&= C_2\alpha + U_2 + \beta_2,
\end{aligned}
\tag{14}
$$

where C_2 and β_2 are similar terms containing the uncertain parameters. They can also be presented by the vectors of the uncertain parameters and the regressors

$$
\begin{aligned}
C_2 &= \theta_3^T\xi_4, \\
\beta_2 &= \theta_3^T\xi_5 + k_{\tilde{\alpha}}\dot{\tilde{\alpha}} - \ddot{\gamma}_d, \\
U_2 &= \theta_4^T\xi_6,
\end{aligned}
\tag{15}
$$

where

$$
\begin{aligned}
\theta_3 &= \left[C_{T,\phi}^{\alpha}; C_T^{\alpha}; C_{T,\phi}^{\alpha M_{\infty}^{-2}}; C_{T,\phi}^{M_{\infty}^{-2}}; C_{T,\phi}^0; C_T^{M_{\infty}^{-2}}; C_T^{A_d}; C_T^0; C_M^{\alpha}; C_M^0 \right], \\[2mm]
\theta_4 &= \left[C_M^{\delta_e}; C_M^{\delta_c} \right], \\[2mm]
\xi_4 &= \frac{\bar{q}}{I_{yy}} \left[z_T\phi; z_T; z_T M_{\infty}^{-2}\phi; 0; 0; 0; 0; 0; S\bar{c}; 0 \right], \\[2mm]
\xi_5 &= \frac{\bar{q}}{I_{yy}} \left[0; 0; 0; z_T M_{\infty}^{-2}\phi; z_T\phi; z_T M_{\infty}^{-2}; z_T A_d; z_T; 0; S\bar{c} \right], \\[2mm]
\xi_6 &= \frac{\bar{q}S\bar{c}}{I_{yy}} \left[\delta_e; \delta_c \right].
\end{aligned}
\tag{16}
$$

So (14) can be reformulated as

$$
\dot{Z} = \theta_3^T\xi_4\alpha + \theta_4^T\xi_6 + \theta_3^T\xi_5 + k_{\tilde{\alpha}}\dot{\tilde{\alpha}} - \ddot{\gamma}_d.
\tag{17}
$$

Due to the uncertainty of the aerodynamic parameters, θ_i, $i = 1, \ldots, 4$ will change with flight of hypersonic vehicles. Therefore it is necessary to estimate their values by the adaptive technique. Let $\hat{\theta}_i$, $\tilde{\theta}_i$ be the estimate vector and the estimate error vector of θ_i, where $\tilde{\theta}_i = \theta_i - \hat{\theta}_i$, $i = 1, \ldots, 4$.

Assumption 1. The aerodynamic parameters θ_i, $i = 1, \ldots, 4$ are bounded; they lie in a compact convex set.

In order to guarantee tracking performance of hypersonic vehicles, the equivalent control inputs U_1 and U_2 are designed, respectively, by replacing the uncertain parameter vector θ_i with its estimate vector and estimate error vector

$$
\begin{aligned}
\widehat{U}_1 &= \hat{\theta}_2^T\xi_3 = -\hat{\theta}_1^T\xi_1\alpha^* - \left(\hat{\theta}_1^T\xi_2 - \frac{g\cos\gamma}{V} - \dot{\gamma}_d \right) \\[2mm]
&\quad + \left(\hat{\theta}_1^T\xi_1 - k_{\tilde{\gamma}} \right)\tilde{\gamma} - V\tilde{h}, \\[2mm]
\widehat{U}_2 &= \hat{\theta}_4^T\xi_6 = \ddot{\gamma}_d - \left(\hat{\theta}_3^T\xi_5 + k_{\tilde{\alpha}}\dot{\tilde{\alpha}} \right) - \hat{\theta}_3^T\xi_4\alpha^* \\[2mm]
&\quad - k_Z Z - \left(\hat{\theta}_3^T\xi_4 + 1 \right)\tilde{\alpha},
\end{aligned}
\tag{18}
$$

where $k_{\tilde{\gamma}} > 0$, $k_Z > 0$ are the design parameters for $\tilde{\gamma}$ and Z.

Let $\delta = [\delta_e, \delta_c]$. There is $\mathbf{U} = B\delta$ according to (7) and (14). B is a coefficient matrix and is equal to $[(\bar{q}S/mV)\hat{\theta}_2^T; (\bar{q}S\bar{c}/I_{yy})\hat{\theta}_4^T]$. The real inputs of the altitude loop can be obtained as follows:

$$
\begin{bmatrix} \delta_e \\ \delta_c \end{bmatrix} = B^{-1}\begin{bmatrix} \widehat{U}_1 \\ \widehat{U}_2 \end{bmatrix}.
\tag{19}
$$

Combining (18), the state error dynamics about the altitude loop is transformed into the following equations:

$$
\begin{aligned}
\dot{\tilde{h}} &\approx -k_{\tilde{h}}\tilde{h} + V\tilde{\gamma}, \\[2mm]
\dot{\tilde{\gamma}} &= -k_{\tilde{\gamma}}\tilde{\gamma} - V\tilde{h} + y_{\tilde{\alpha}} + \tilde{\theta}_1^T\xi_1\alpha + \tilde{\theta}_1^T\xi_2 + \tilde{\theta}_2^T\xi_3, \\[2mm]
\dot{\tilde{\alpha}} &= Z - k_{\tilde{\alpha}}\tilde{\alpha}, \\[2mm]
\dot{Z} &= -k_Z Z - \tilde{\alpha} + y_{\tilde{\gamma}} + \tilde{\theta}_3^T\xi_4\alpha + \tilde{\theta}_3^T\xi_5 + \tilde{\theta}_4^T\xi_6,
\end{aligned}
\tag{20}
$$

where $y_{\tilde{\alpha}} = \tilde{\theta}_1^T\xi_1\tilde{\alpha}$, $y_{\tilde{\gamma}} = -\tilde{\theta}_3^T\xi_4\tilde{\gamma}$.

For ensuring the stability of the altitude loop, the new formulation (20) is divided into the altitude-flight-path angle subsystem and the attack angle-pitch rate subsystem. As illustrated in Figure 1, these two subsystems constitute a structure of interconnection. It is seen that $y_{\tilde{\alpha}}$ and $y_{\tilde{\gamma}}$ act as the input and output of the altitude-flight-path angle subsystem and $y_{\tilde{\gamma}}$, $y_{\tilde{\alpha}}$ are the input and output of the attack angle-pitch rate subsystem, respectively.

For the above interconnection subsystems, input-to-state stability will be analyzed via small gain theorem. Firstly, the definition of the asymptotic L_∞ norm $\|\cdot\|_a$ is given [19]

$$
\|\lambda\|_a := \lim_{t\to\infty}\sup|\lambda|.
\tag{21}
$$

Then, define $\psi_1 = \sqrt{\tilde{h}^2 + \tilde{\gamma}^2}$, and choose the Lyapunov function candidate of the altitude-flight-path angle subsystem as

$$
W_1 = \frac{1}{2}\left(\tilde{h}^2 + \tilde{\gamma}^2 \right) + \frac{1}{2}\tilde{\theta}_1^T\tau_1^{-1}\tilde{\theta}_1 + \frac{1}{2}\tilde{\theta}_2^T\tau_2^{-1}\tilde{\theta}_2.
\tag{22}
$$

Its time derivative is

$$
\begin{aligned}
\dot{W}_1 &= \tilde{h}\dot{\tilde{h}} + \tilde{\gamma}\dot{\tilde{\gamma}} - \tilde{\theta}_1^T\tau_1^{-1}\dot{\hat{\theta}}_1 - \tilde{\theta}_2^T\tau_2^{-1}\dot{\hat{\theta}}_2 \\[2mm]
&= -k_{\tilde{h}}\tilde{h}^2 - k_{\tilde{\gamma}}\tilde{\gamma}^2 + \tilde{\gamma}y_{\tilde{\alpha}} + \tilde{\theta}_1^T\tau_1^{-1}\left\{ \tau_1\tilde{\gamma}(\xi_1\alpha + \xi_2) - \dot{\hat{\theta}}_1 \right\} \\[2mm]
&\quad + \tilde{\theta}_2^T\tau_2^{-1}\left(\tau_2\tilde{\gamma}\xi_3 - \dot{\hat{\theta}}_2 \right).
\end{aligned}
\tag{23}
$$
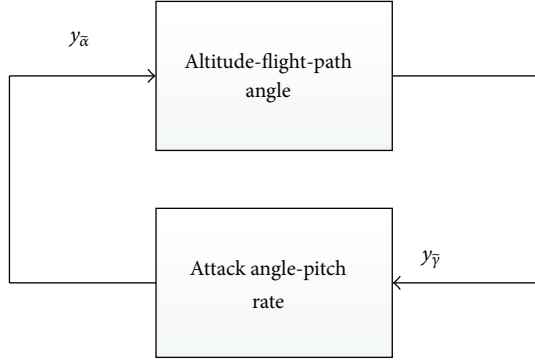
FIGURE 1: Interconnection subsystem structure.

The adaptive laws of $\widehat{\theta}_1$, $\widehat{\theta}_2$ are designed as

$$\dot{\widehat{\theta}}_1 = \tau_1 \widetilde{\gamma} (\xi_1 \alpha + \xi_2),$$
$$\dot{\widehat{\theta}}_2 = \tau_2 \widetilde{\gamma} \xi_3, \tag{24}$$

where τ_1 and τ_2 are the adaptive parameters.

By (24), (23) becomes

$$\dot{W}_1 \leq -\min\left\{k_{\widetilde{h}}, k_{\widetilde{\gamma}}\right\} |\psi_1|^2 + |\psi_1| |y_{\widetilde{\alpha}}|. \tag{25}$$

As a consequence, it satisfies W_1 which is negative definite when $|\psi_1| \geq |y_{\widetilde{\alpha}}| / \min\{k_{\widetilde{h}}, k_{\widetilde{\gamma}}\}$. Then W_1 is a input-to-state stable Lyapunov function. According to the lemma in [19], we know that $\|\psi_1\|_a \leq \|y_{\widetilde{\alpha}}\|_a / \min\{k_{\widetilde{h}}, k_{\widetilde{\gamma}}\}$. As $y_{\widetilde{\gamma}} = -\widehat{\theta}_3^T \xi_4 \widetilde{\gamma}$, the following formulation is obtained:

$$\left\|y_{\widetilde{\gamma}}\right\|_a = \left\|-\widehat{\theta}_3^T \xi_4 \widetilde{\gamma}\right\|_a \leq \widehat{\theta}_3^T \xi_4 \|\psi_1\|_a \leq \frac{\widehat{\theta}_3^T \xi_4}{\min\left\{k_{\widetilde{h}}, k_{\widetilde{\gamma}}\right\}} \|y_{\widetilde{\alpha}}\|_a. \tag{26}$$

For the attack angle-pitch rate subsystem, $\psi_2 = \sqrt{\widetilde{\alpha}^2 + Z^2}$ is defined, and the following Lyapunov function candidate is chosen:

$$W_2 = \frac{1}{2}\left(\widetilde{\alpha}^2 + Z^2\right) + \frac{1}{2}\widetilde{\theta}_3^T \tau_3^{-1} \widetilde{\theta}_3 + \frac{1}{2}\widetilde{\theta}_4^T \tau_4^{-1} \widetilde{\theta}_4. \tag{27}$$

Its time derivative is

$$\dot{W}_2 = \widetilde{\alpha}\dot{\widetilde{\alpha}} + Z\dot{Z} - \widetilde{\theta}_3^T \tau_3^{-1}\dot{\widehat{\theta}}_3 - \widetilde{\theta}_4^T \tau_4^{-1}\dot{\widehat{\theta}}_4$$
$$= -k_{\widetilde{\alpha}}\widetilde{\alpha}^2 + k_Z Z^2 + Z y_{\widetilde{\gamma}} + \widetilde{\theta}_3^T \tau_3^{-1}\left\{\tau_3 Z(\xi_4 \alpha + \xi_5) - \dot{\widehat{\theta}}_3\right\}$$
$$+ \widetilde{\theta}_4^T \tau_4^{-1}\left(\tau_4 Z\xi_6 - \dot{\widehat{\theta}}_4\right), \tag{28}$$

where the adaptive laws of $\widehat{\theta}_3$, $\widehat{\theta}_4$ are determined as

$$\dot{\widehat{\theta}}_3 = \tau_3 Z(\xi_4 \alpha + \xi_5),$$
$$\dot{\widehat{\theta}}_4 = \tau_4 Z\xi_6. \tag{29}$$

Substituting (29) in (28), we can acquire

$$\dot{W}_2 \leq -\min\left\{k_{\widetilde{\alpha}}, k_Z\right\} |\psi_2|^2 + |\psi_2| |y_{\widetilde{\gamma}}|. \tag{30}$$

When $|\psi_2| \geq |y_{\widetilde{\gamma}}| / \min\{k_{\widetilde{\alpha}}, k_Z\}$, $\dot{W}_2 \leq 0$. Similarly, $\|\psi_2\|_a \leq \|y_{\widetilde{\gamma}}\|_a / \min\{k_{\widetilde{\alpha}}, k_Z\}$ can be obtained, and W_2 is input-to-state stable as well. Because $y_{\widetilde{\alpha}} = \widehat{\theta}_1^T \xi_1 \widetilde{\alpha}$, there is

$$\|y_{\widetilde{\alpha}}\|_a = \left\|\widehat{\theta}_1^T \xi_1 \widetilde{\alpha}\right\|_a \leq \widehat{\theta}_1^T \xi_1 \|\psi_2\|_a \leq \frac{\widehat{\theta}_1^T \xi_1}{\min\left\{k_{\widetilde{\alpha}}, k_Z\right\}} \|y_{\widetilde{\gamma}}\|_a. \tag{31}$$

The interconnection formulation (20) is input-to-state stable according to small-gain theorem if we choose proper design parameters to make the following equation holds

$$\frac{\widehat{\theta}_3^T \xi_4}{\min\left\{k_{\widetilde{h}}, k_{\widetilde{\gamma}}\right\}} \cdot \frac{\widehat{\theta}_1^T \xi_1}{\min\left\{k_{\widetilde{\alpha}}, k_Z\right\}} < 1. \tag{32}$$

Therefore the tracking errors and estimate errors of the altitude loop can converge to a small neighborhood of origin.

3.2. Velocity Controller. Since velocity is controlled by ϕ directly, the adaptive dynamic inversion method is used. Let $\widetilde{V} = V - V_{\text{ref}}$; the error dynamics of velocity is written as

$$\dot{\widetilde{V}} = \frac{T\cos\alpha - D}{m} - g\sin\gamma - \dot{V}_{\text{ref}}$$
$$= \frac{\overline{q}\left(C_{T,\phi}\phi + C_T\right)\cos\alpha - \overline{q}SC_D}{m} - g\sin\gamma - \dot{V}_{\text{ref}}. \tag{33}$$

For existence of uncertain parameters, the following vectors and repressors are defined

$$\theta_5 = \left[C_D^{(\alpha+\Delta\tau_1)}; C_D^{(\alpha+\Delta\tau_1)^2}; C_D^{\delta_e^2}; C_D^{\delta_e}; C_D^{\delta_c^2}; C_D^{\delta_c};\right.$$
$$\left. C_D^{\alpha\delta_e}; C_D^{\alpha\delta_c}; C_D^0; C_T^{A_d}; C_T^\alpha; C_T^{M_\infty^{-2}}; C_T^0\right],$$
$$\theta_6 = \left[C_{T,\phi}^\alpha; C_{T,\phi}^{\alpha M_\infty^{-2}}; C_{T,\phi}^{M_\infty^{-2}}; C_{T,\phi}^0\right],$$
$$\xi_7 = \overline{q}\left[S\alpha; S\alpha^2; S\delta_e^2; S\delta_e; S\delta_c^2; S\delta_c; S\alpha\delta_e; S\alpha\delta_c; S;\right.$$
$$\left. -A_d\cos\alpha; -\alpha\cos\alpha; -M_\infty^{-2}\cos\alpha; -\cos\alpha\right],$$
$$\xi_8 = \overline{q}\cos\alpha\left[\alpha; \alpha M_\infty^{-2}; M_\infty^{-2}; 1\right]. \tag{34}$$

Consequently,

$$\dot{\widetilde{V}} = \frac{\theta_6^T \xi_8 \phi - \theta_5^T \xi_7}{m} - g\sin\gamma - \dot{V}_{\text{ref}}. \tag{35}$$

Then the control input ϕ is designed as

$$\phi = \frac{-mk_{\widetilde{v}}\widetilde{V} + m\dot{V}_{\text{ref}} + mg\sin\gamma + \widehat{\theta}_5^T \xi_7}{\widehat{\theta}_6^T \xi_8}, \tag{36}$$

where $k_{\widetilde{v}} > 0$ is a design parameter.

(a) Altitude

(b) Velocity

(c) Attack angle

(d) Flight-path angle

(e) Flexible states

(f) Fuel-to-air ratio
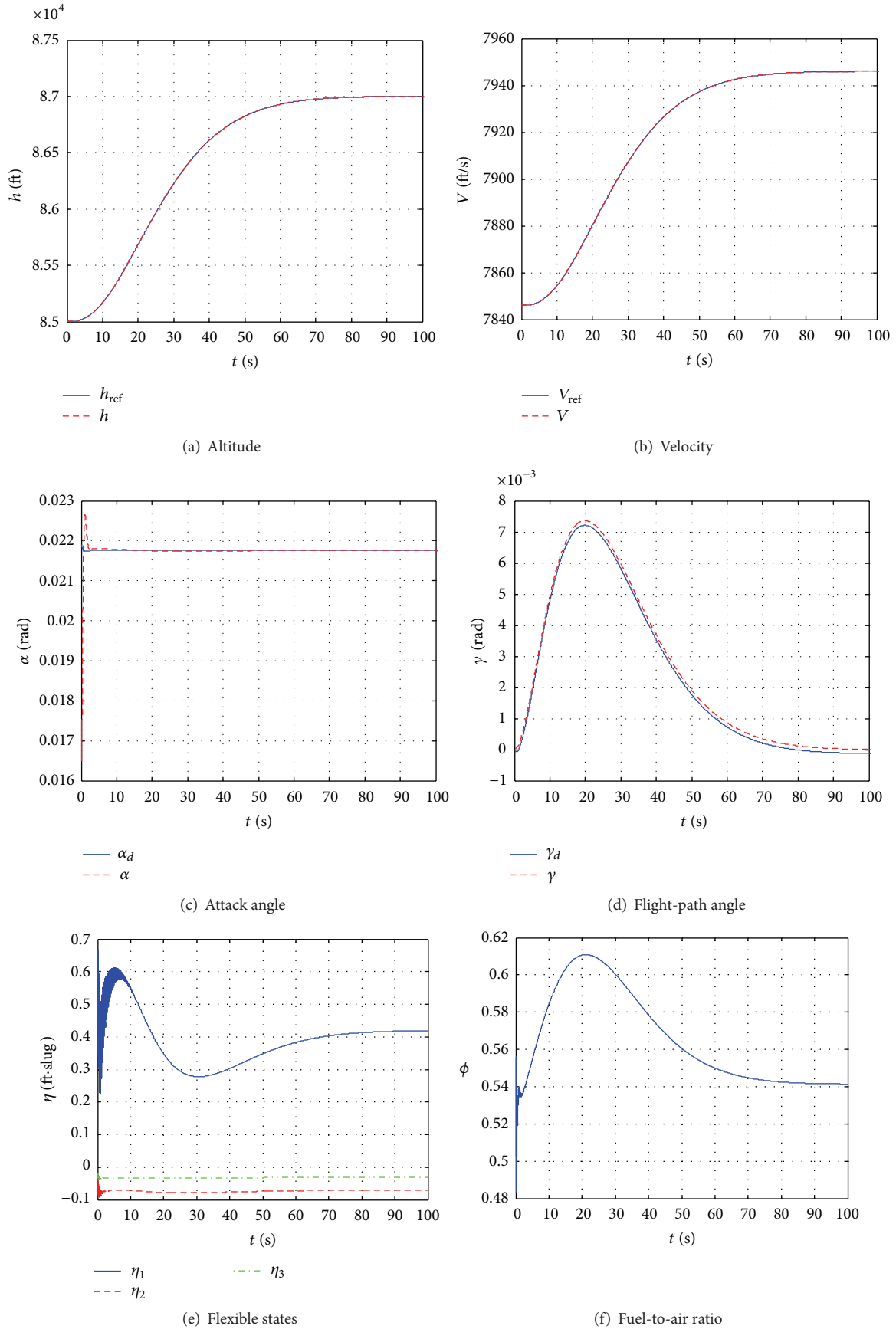
FIGURE 2: Continued.
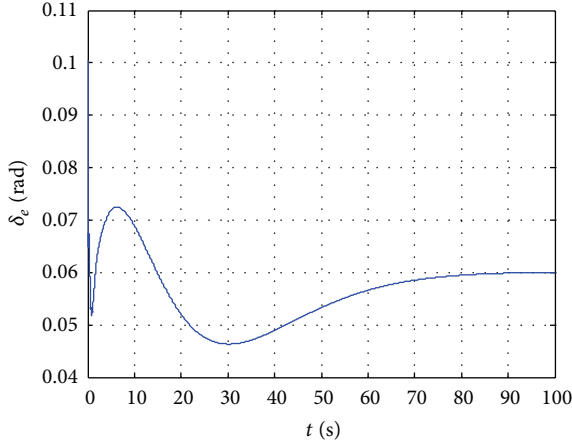
(g) Elevator deflection
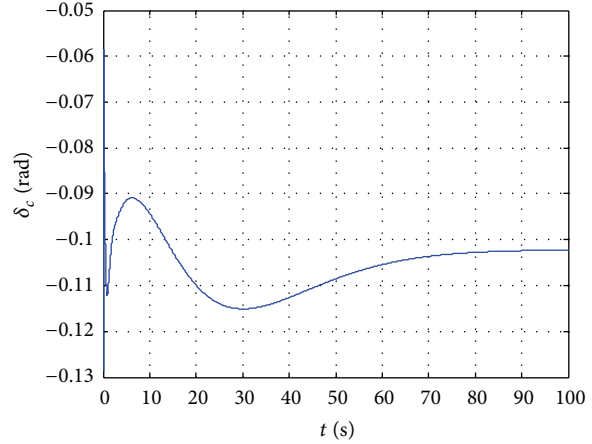
(h) Canard deflection

Figure 2: Climbing maneuver with longitudinal acceleration for case one.

Determine the Lyapunov function candidate as

$$W_3 = \frac{1}{2}m\widetilde{V}^2 + \frac{1}{2}\widetilde{\theta}_5^T \tau_5^{-1}\widetilde{\theta}_5 + \frac{1}{2}\widetilde{\theta}_6^T \tau_6^{-1}\widetilde{\theta}_6. \tag{37}$$

Its time derivative is

$$\begin{aligned}
\dot{W}_3 &= \widetilde{V}\left(\theta_6^T \xi_8 \phi - \theta_5^T \xi_7 - mg\sin\gamma - m\dot{V}_{\text{ref}}\right) \\
&\quad - \widetilde{\theta}_5^T \tau_5^{-1}\dot{\hat{\theta}}_5 - \widetilde{\theta}_6^T \tau_6^{-1}\dot{\hat{\theta}}_6 \\
&= \widetilde{V}\left(\theta_6^T \xi_8 \phi - mk_{\widetilde{v}}\widetilde{V} - \widetilde{\theta}_5^T \xi_7\right) - \widetilde{\theta}_5^T \tau_5^{-1}\dot{\hat{\theta}}_5 - \widetilde{\theta}_6^T \tau_6^{-1}\dot{\hat{\theta}}_6 \\
&= -mk_{\widetilde{v}}\widetilde{V}^2 - \widetilde{\theta}_5^T \tau_5^{-1}\left(\tau_5\widetilde{V}\xi_7 + \dot{\hat{\theta}}_5\right) + \widetilde{\theta}_6^T \tau_6^{-1}\left(\tau_6\phi\xi_8 - \dot{\hat{\theta}}_6\right).
\end{aligned} \tag{38}$$

The adaptive laws of $\hat{\theta}_5$, $\hat{\theta}_6$ are obtained in the following:

$$\begin{aligned}
\dot{\hat{\theta}}_5 &= -\tau_5\widetilde{V}\xi_7, \\
\dot{\hat{\theta}}_6 &= \tau_6\phi\xi_8.
\end{aligned} \tag{39}$$

Thus (38) becomes $\dot{W}_3 = -mk_{\widetilde{v}}\widetilde{V}^2 < 0$; that is, when $t \to \infty$, the tracking errors and estimate errors of the velocity subsystem can converge to zero finally.

Therefore the accurate tracking performance and the stability of altitude and velocity can be guarranteed by the proposed method.

4. Numerical Simulation

The feasibility of the proposed method is verified based on a flexible model (1)–(3). The initial trim conditions are $h = 85000$ ft, $V = 7846$ ft/s, $\alpha = 0.0174$ rad, $\gamma = 0$ rad, $q = 0$ rad/s, $\eta_1 = 0.4588$ ft·sulg, $\eta_2 = -0.08726$ ft·sulg, and $\eta_3 = -0.03671$ ft·sulg. Two cases are studied here.

Case one is a climbing maneuver with longitudinal acceleration, and the expected equilibrium is $\alpha^* = 0.0219$ rad.

The increments of altitude and velocity are 2000 ft, and 100 ft/s respectively. Case two is a descending maneuver with velocity reducing gradually, and its corresponding equilibrium is $\alpha^* = 0.0158$ rad. The decreasing of altitude is 1000 ft and that of velocity is 100 ft/s.

For these two cases, The corresponding reference commands are generated by filtering step reference commands with a second-order profiler with $\omega = 0.1$ rad/s and $\xi = 0.9$.

The simulation results of case one are shown in Figure 2.

The simulation results of case two are shown in Figure 3.

From Figures 2(a), 2(b), 3(a), and 3(b), it is seen that the controller can provide stable and accurate tracking of the reference trajectories for the two cases, and the tracking errors of altitude and velocity remain remarkably small. Figures 2(c), 2(d), 3(c), and 3(d) show that both the signals of the flight-path angle and the attack angle can also follow the change of virtual control commands closely.

For the flexible dynamics, its effect on aerodynamic model is neglected, and its motion is taken as external perturbation during the control design. That means that the forebody turn angle $\Delta\tau_1$ and the aftbody vertex angle $\Delta\tau_2$ are equal to zero in model (3) when the controller is designed. Simultaneously, the second-order equation about flexible states η_i and $\dot{\eta}_i$ is not considered. From Figures 2(e) and 3(e), we can know that the flexible states can converge to stable states ultimately although the flexible dynamics is not taken into account directly. This denotes that our controller has the strong robustness, and it is suitable to control the flexible hypersonic vehicle.

Moreover, the variation ranges of the control inputs that is, fuel-to-air ratio, elevator deflection, and canard deflection are bounded according to Figures 2(f), 2(g), 2(h), 3(f), 3(g), and 3(h).

In summary, the nonminimum phase behavior is suppressed successfully, and the excellent closed-loop behavior of air-breathing hypersonic vehicle can be obtained by the proposed controller for the cases of maneuver of altitude and velocity.
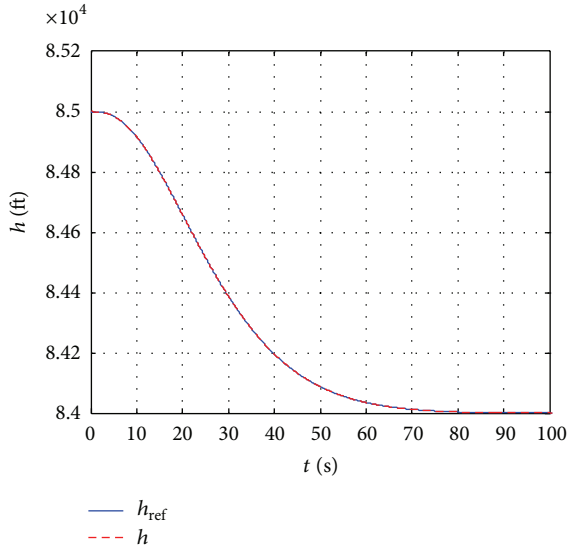
(a) Altitude
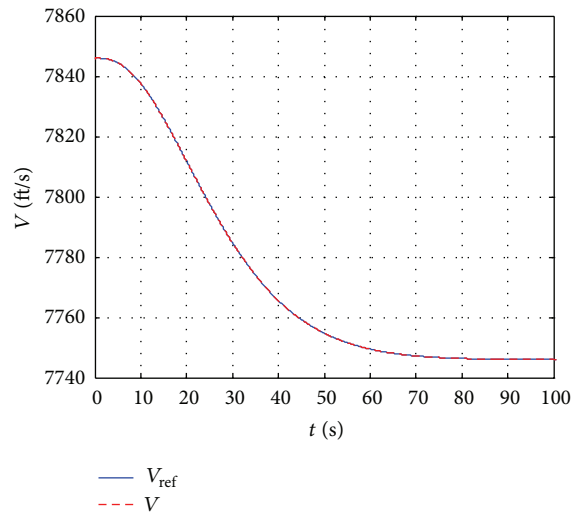
(b) Velocity
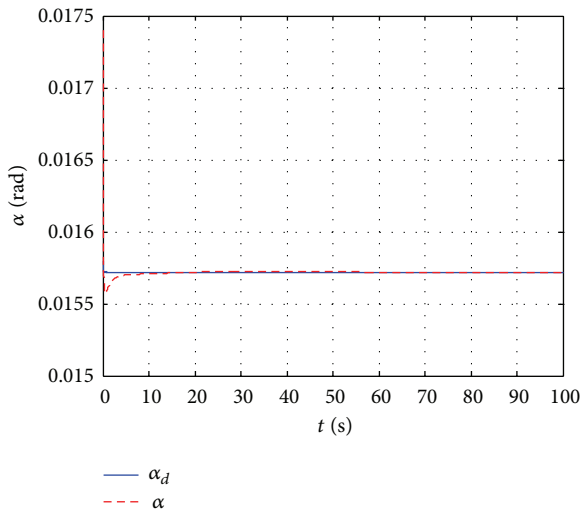
(c) Attack angle
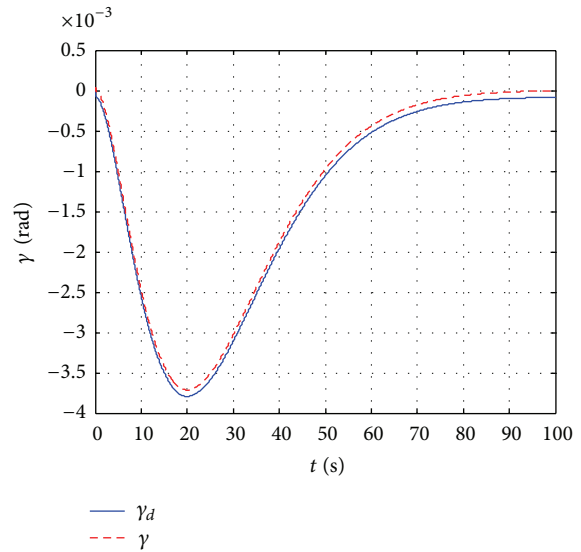
(d) Flight-path angle
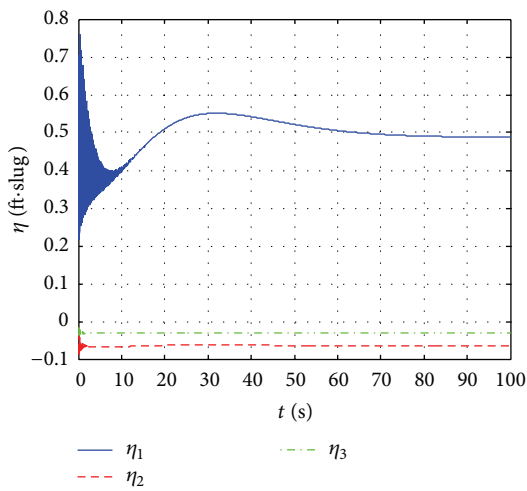
(e) Flexible states
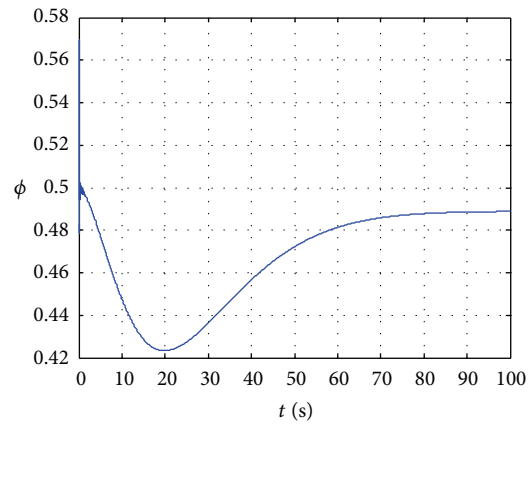
(f) Fuel-to-air ratio

FIGURE 3: Continued.

(g) Elevator deflection

(h) Canard deflection
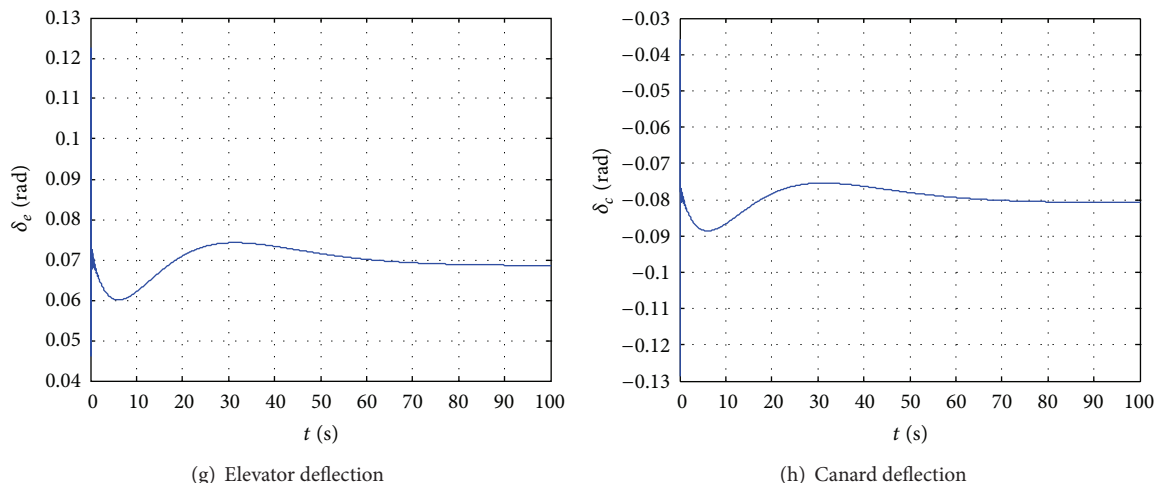
FIGURE 3: Descending maneuver with velocity reducing gradually for case two.

5. Conclusion

For the flexible air-breathing hypersonic vehicle with canard control surface, the controller is designed based on the nonlinear adaptive equivalent control strategy under interconnected structure. The equivalent control inputs are introduced and designed to replace the terms about elevator and canard in the flight-path angle dynamics and the pitch-rate dynamics for eliminating the nonminimum phase. The uncertain aerodynamic parameters are identified online by the adaptive method. And input-to-state stability of the interconnection subsystems is guaranteed by small-gain theorem. Similarly, the adaptive dynamic inversion approach is adopted in the velocity loop. With our approach, the stable and accurate tracking of the hypersonic vehicle model with nonminimum phase can be realized.

Acknowledgments

References

[1] M. A. Bolender and D. B. Doman, "Nonlinear longitudinal dynamical model of an air-breathing hypersonic vehicle," *Journal of Spacecraft and Rockets*, vol. 44, no. 2, pp. 374–387, 2007.

[2] J. T. Parker, A. Serrani, S. Yurkovich, M. A. Bolender, and D. B. Doman, "Control-oriented modeling of an air-breathing hypersonic vehicle," *Journal of Guidance, Control, and Dynamics*, vol. 30, no. 3, pp. 856–869, 2007.

[3] B. Fidan, M. Kuipers, P. A. Ioannou, and M. Mirmirani, "Longitudinal motion control of air-breathing hypersonic vehicles based on time-varying models," in *Proceedings of the 14th AIAA/AHI International Space Planes and Hypersonics Systems Technologies Conference*, pp. 1705–1717, AIAA, Canberra, Australia, November 2006.

[4] K. P. Groves, D. O. Sigthorsson, A. Serrani, S. Yurkovich, M. A. Bolender, and D. B. Doman, "Reference command tracking for a linearized model of an air-breathing hypersonic vehicle," in *Proceedings of the AIAA Guidance, Navigation, and Control Conference*, pp. 2901–2914, AIAA, San Francisco, Calif, USA, August 2005.

[5] D. O. Sigthorsson, P. Jankovsky, A. Serrani, S. Yurkovich, M. A. Bolender, and D. B. Doman, "Robust linear output feedback control of an airbreathing hypersonic vehicle," *Journal of Guidance, Control, and Dynamics*, vol. 31, no. 4, pp. 1052–1066, 2008.

[6] L. G. Wu, X. B. Yang, and F. B. Li, "Nonfragile output tracking control of hypersonic air-breathing vehicles with LPV model," *IEEE/ASME Transactions on Mechatronics*, vol. 18, no. 4, pp. 1280–1288, 2013.

[7] H. P. Lee, S. E. Reiman, C. H. Dillon, and H. M. Youssef, "Robust nonlinear dynamic inversion control for a hypersonic cruise vehicle," in *Proceedings of the AIAA Guidance, Navigation, and Control Conference and Exhibit*, pp. 3380–3388, Hilton Head, SC, USA, August 2007.

[8] H. J. Xu, M. D. Mirmirani, and P. A. Ioannou, "Adaptive sliding mode control design for a hypersonic flight vehicle," *Journal of Guidance, Control, and Dynamics*, vol. 27, no. 5, pp. 829–838, 2004.

[9] B. L. Tian, Q. Zong, J. Wang, and F. Wang, "Quasi-continuous high-order sliding mode controller design for reusable launch vehicles in reentry phase," *Aerospace Science and Technology*, vol. 28, no. 1, pp. 198–207, 2013.

[10] B. Xu, F. Sun, H. Liu, and J. Ren, "Adaptive Kriging controller design for hypersonic flight vehicle via back-stepping," *IET Control Theory and Applications*, vol. 6, no. 4, pp. 487–497, 2012.

[11] T. E. Gibson, L. G. Crespo, and A. M. Annaswamy, "Adaptive control of hypersonic vehicles in the presence of modeling uncertainties," in *Proceedings of the 2009 American Control Conference (ACC '09)*, pp. 3178–3183, St. Louis, Mo, USA, June 2009.

[12] H. Buschek and A. J. Calise, "Uncertainty modeling and fixed-order controller design for a hypersonic vehicle model," *Journal*

of Guidance, Control, and Dynamics, vol. 20, no. 1, pp. 42–48, 1997.

[13] Q. Wang and R. F. Stengel, "Robust nonlinear control of a hypersonic aircraft," *Journal of Guidance, Control, and Dynamics*, vol. 23, no. 4, pp. 577–585, 2000.

[14] J. Yang, S. H. Li, C. Y. Sun, and L. Guo, "Nonlinear-disturbance-observer-based robust flight control for airbreathing hypersonic vehicles," *IEEE Transactions on Aerospace and Electronic Systems*, vol. 49, no. 2, pp. 1263–1275, 2013.

[15] L. Fiorentini, A. Serrani, M. A. Bolender, and D. B. Doman, "Nonlinear robust/adaptive controller design for an airbreathing hypersonic vehicle model," in *Proceedings of the AIAA Guidance, Navigation, and Control Conferenc and Exhibit*, pp. 269–284, AIAA, Hilton Head, SC, USA, August 2007.

[16] L. Fiorentini, A. Serrani, M. A. Bolender, and D. B. Doman, "Nonlinear robust adaptive control of flexible air-breathing hypersonic vehicles," *Journal of Guidance, Control, and Dynamics*, vol. 32, no. 2, pp. 401–416, 2009.

[17] L. Fiorentini, A. Serrani, M. A. Bolender, and D. B. Doman, "Nonlinear control of nonminimum phase hypersonic vehicle models," in *Proceedings of the 2009 American Control Conference (ACC '09)*, pp. 3160–3165, St. Louis, Mo, USA, June 2009.

[18] D. O. Sigthorsson and A. Serrani, "Development of linear parameter-varying models of hypersonic air-breathing vehicles," in *Proceedings of the AIAA Guidance, Navigation, and Control Conference and Exhibit*, pp. 2009–6282, AIAA, Chicago, Ill, USA, August 2009.

[19] A. R. Teel, "A nonlinear small gain theorem for the analysis of control systems with saturation," *IEEE Transactions on Automatic Control*, vol. 41, no. 9, pp. 1256–1270, 1996.